Theo Peschke[1,2]
Patrick Bitterwolf[1]
Kersten S. Rabe[1]
Christof M. Niemeyer[1,*]

Self-Immobilizing Oxidoreductases for Flow Biocatalysis in Miniaturized Packed-Bed Reactors

The industrial implementation of enzymes in flow biocatalysis microreactors is expected to be essential for the emergence of a bio-based circular economy. Major challenges concern the efficient immobilization of delicate enzymes inside miniaturized reactors without compromising their catalytic activity. We describe the exploitation of the widely used His-tag system in a microfluidic packed-bed reactor that contains ketoreductase-functionalized magnetic beads. In a continuous process, these reactors produced highly stereoselective (*R*)-configured alcohols (d.r. 99:1) with an average conversion of > 90 % for more than 4 days. We believe that such miniaturized flow reactors can be of great utility for future sustainable production processes.

Keywords: Biocatalysis, Enzymes, Immobilization techniques, Microreactors, Stereoselective reactions

1 Introduction

Enzymes are powerful natural catalysts that have been perfectly tuned by evolution to accelerate a specific reaction, often much more efficiently than catalysts for the same reaction developed by man. Their industrial implementation is expected to have an enormous impact on the emergence of a bio based circular economy or "bioeconomy" with a net carbon emission of zero, resulting in sustainable synthesis processes for the efficient conversion of renewable biomass as an alternative to petro chemicals [1]. Recent progress in the implementation of bio catalysts for the production of pharmaceutical drugs, such as Ipatasertib (Roche) [2], Montelukast (Singulair® by Merck Sharp & Dohme) [3], Atorvastatin (Sortis®, Atorvalan®, or Lipitor® by Pfizer) [4], or Sitagliptin (Merck Sharp & Dohme) [5], clearly indicates the applicability of this approach to indus trial production processes [6]. However, further improvement of this approach will crucially depend on the availability of flexible and robust technical production platforms. Towards this end, a rich source of innovation for modular production processes is currently drawn from biological means for the compartmentalization and cascading of multiple enzymatic transformations [7 16]. One important approach to implement enzyme cascades into future biocatalytic processes takes advantage of compartmentalized microfluidic reactors. These microreactors offer a high level of control over temperature profiles and diffusion based mixing [17, 18]. However, a major challenge for the establishment of flow biocatalysis in micro reactors concerns the immobilization of isolated enzymes [19]. In many cases, purified enzymes are immobilized through sim ple non specific physisorption on charged carrier particles. However, this approach can lead to a strong decrease or even total loss of enzymatic activity [18, 19]. Several less harsh immobilization strategies rely on enzymes that are chemically tagged with affinity ligands, such as biotin [20, 21] or DNA oligonucleotides [22]. Since such approaches require additional efforts for chemical modification and purification of the enzymes, we have recently established a set of genetically encoded tags for enzyme immobilization [23 25]. These are based on mild orthogonal coupling systems, such as the strep tavidin binding peptide (SBP) tag [26], the SpyTag/SpyCatcher (ST/SC) system [27], or a variant of the Halo tag system [28] dubbed as HOB (Halo based oligonucleotide binder) [29]. In deed, the self immobilizing enzymes can be used even directly from crude cell extracts [23, 24], and the feasibility of this approach was recently confirmed for Halo tagged enzymes [30, 31]. Moreover, silica binding modules (SBM, also dubbed as Z_{basic2} tag) can be genetically engineered into enzymes of interest to enable their immobilization on silica substrates, such as, e.g., borosilicate glass [32].

However, in the light of these recent developments, it is also necessary to consider established protein tags, such as the hexahistidine (His) tag, which is widely applied in affinity puri fication of recombinant proteins. Despite several drawbacks

[1]Dr. Theo Peschke, M.Sc. Patrick Bitterwolf, Dr. Kersten S. Rabe, Prof. Dr. Christof M. Niemeyer
niemeyer@kit.edu
Karlsruhe Institute of Technology (KIT), Institute for Biological Interfaces (IBG 1), Hermann von Helmholtz Platz 1, 76344 Eggen stein Leopoldshafen, Germany.

[2]Dr. Theo Peschke
Current address: Novartis AG, Kohlestrasse WSJ 103, 4002 Basel, Switzerland.

associated with His tag immobilization, such as a relatively low affinity ($K_d \sim 3\,\mu M$) [33] and specificity [34], as well as poten tially adverse effects on the activity of enzymes containing diva lent metal ions [35], this approach has been successfully applied to one step purification and immobilization to generate enzymatic cascade reactions in microchips [36 39], on microbeads [40 42], or on polymer coated controlled porous glass beads (EziG^{TM}) [43 45]. Other advantages of the His tag include its short six amino acid sequence that can be intro duced conveniently in a single polymerase chain reaction (PCR) step and the variety of well established and commer cially available equipment for purification and analysis. To ena ble direct comparison of the well established His tag with the recently described self immobilization systems [23, 24], we here report on the use of His tagged oxidoreductases for flow biocatalysis in miniaturized packed bed reactors loaded with enzyme functionalized magnetic beads (MB) (Fig. 1). We employed the highly (*R*) stereoselective ketoreductase LbADH (alcohol dehydrogenase from *Lactobacillus brevis*), in combina tion with a glucose dehydrogenase (GDH) for continuous cofactor regeneration, for setting up microfluidic packed bed reactors that produce highly stereoselective (*R*) configured alcohols in a continuous process for more than 4 days.

2 Experimental

2.1 Cloning of Plasmids

The cloning of the expression plasmids for His LbADH and GDH His was done as previously described [25].

2.2 Expression, Purification, and Characterization of Enzymes

Expression, purification, and characterization of the proteins were done as previously described [24, 25]. In brief, *Escherichia coli* BL21(DE3) cells were transformed with the corresponding expression vectors using electroporation. The freshly trans formed *E. coli* cells harboring the plasmids were selected overnight on Luria Bertani (LB)/agar plates supplemented with $100\,\mu g\,mL^{-1}$ ampicillin at 37 °C. Liquid cultures of 20 mL LB medium containing ampicillin were started from the overnight plate cultures. The cultures were incubated for 14 18 h at 37 °C, 180 rpm in a 150 mL shaking flask and were then trans ferred into 4 L shaking flasks with 2 L LB medium containing ampicillin and incubated at 37 °C, 180 rpm until the optical density at 600 nm (OD_{600}) reached a value of 0.6. The tempera ture was then lowered to 25 °C and isopropyl β d 1 thiogalac topyranoside (IPTG) was added to the media in a final concen tration of 0.1 mM for an additional 16 h. The cells were harvested by centrifugation (10 000×*g*, 10 min) and resus pended in 30 mL buffer A (50 mM NaH_2PO_4, 300 mM NaCl, 1 mM $MgCl_2$, 10 mM imidazole, pH 8.0). After disruption of the cell membrane by ultrasonication, the cell lysate was obtained by centrifugation (45 000×*g*, 1 h), filtered through a 0.45 µm Durapore polyvinylidene fluoride (PVDF) membrane (Steriflip, Millipore) and loaded on a HisTrap FF (5 mL) Ni^{2+} nitrilotriacetic acid (NTA) immobilized metal affinity chroma tography (IMAC) column (GE Healthcare, Germany) mounted on an Äkta Pure liquid chromatography system (GE Health care, Germany). The column was washed with 50 mL of buffer A and the His tagged GDH and LbADH were eluted with 100 % buffer B (50 mM NaH_2PO_4, 300 mM NaCl, 500 mM imidazole, pH 8.0). Subsequently, the buffer was exchanged to KP_i Mg (100 mM K_2HPO_4/KH_2PO_4 pH 7.5, 1 mM $MgCl_2$) by Vivaspin 10 000 MWCO (molecular weight cut off; GE Health care). The purity of the recombinant, purified proteins was analyzed by standard discontinuous sodium dodecylsulfate (SDS) polyacrylamide Laemmli midi gels, visualized by Coomassie staining. The protein concentrations were deter mined by UV Vis spectroscopy, using the theoretical molar extinction coefficients at 280 nm, as calculated by the Geneious software version 8.0.5 [46].

2.3 Enzyme Immobilization on Magnetic Microbeads

Per milligram of the MB (Dynabeads^{TM} His tag Isolation and Pulldown from Thermo Fisher Scientific), 1 nmol of His LbADH or GDH His was mixed for 30 min at 30 °C in a tube rotator. The MB were subsequently washed three times with KP_i Mg supplemeted with 0.01 % Tween 20 (KP_i Mg T).

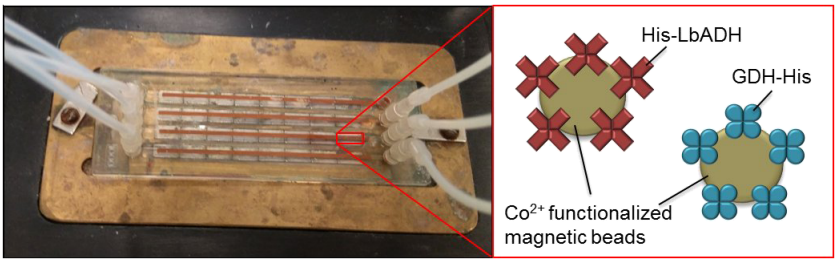

Figure 1. Compartmentalized microfluidic packed-bed reactor loaded with enzyme-functionalized magnetic beads. The four-channel PMMA chip is mounted on a tempera-ture-controlled chip holder which serves as chip-to-world interface. Rectangular Nd magnets underneath the channel compartments retain the enzyme-functionalized superparamagnetic beads inside the reactor. The beads are functionalized with Co^{2+}, for selective binding of the His-tagged enzymes, GDH-His or His-LbADH.

2.4 Determination of Enzyme Activity

Determination of enzyme activity was car ried out as previously described [24, 25]. In brief, the reaction mixtures contained 5 mM 5 nitrononane 2,8 dione (NDK) **1** in KP_i Mg T supplemented with 100 mM glucose, 1 mM $NADP^+$ and an excess of 10 µM GDH His for the determination of the average specific activity of free and immobilized His LbADH. The mixture was preincubated for at least 30 min at 30 °C, before the reaction was started by adding 0.5 µM His LbADH or 200 µg enzyme

functionalized His LbADH@MB Co^{2+}. The mixtures were incubated for 20 min at 30 °C, 1000 rpm in a 2 mL reaction cup. In order to measure the GDH His activity, 0.5 µM GDH His or 200 µg GDH His@MB Co^{2+} was incubated together with an excess of 10 µM His LbADH, using the same conditions as described above. Samples were taken manually at variable time intervals and analyzed by chiral high performance liquid chromatography (HPLC).

2.5 Determination of the MB Binding Capacity

For SDS gel analysis of the protein binding capacity of MB Co^{2+}, the non covalent immobilization of the His tag with Co^{2+} on the bead surface was first disrupted by heating 125 µg enzyme functionalized beads in 1 % (v/v) SDS for 10 min at 95 °C. The supernatant from the denatured MB samples was purified by magnetic separation and analyzed by standard discontinuous SDS polyacrylamide Laemmli midi gels. The bands were visualized by Coomassie staining and compared to the PageRuler™ prestained protein ladder plus (Thermo Scientific) as well as with calibration samples that contained predefined amounts of the corresponding purified protein (0.25, 0.5, 1, and 2 µg). The comparative greyscale analysis was performed with the ImageJ 1.48v software [47].

2.6 Microfluidic Experiments

The microfluidic particle reactors were prepared as previously described [24]. In brief, the enzyme functionalized MB Co^{2+} were loaded into the individual compartments of a polymethyl methacrylate (PMMA) chip (microfluidic ChipShop, Jena, Germany) comprising four linear flow channels that can be connected with each other by conventional polytetrafluoro ethylene (PTFE) tubing. The chipholder was equipped with eight Nd permanent magnets, positioned underneath each of the channels of the chip. Filling of the compartments with bead suspension was achieved through a Mini Luer to pipette adapter through an inserted pipette tip using a negative flow rate of 50 µL min^{-1}. This led to the formation of a non homogenously distributed layer of MB induced by the non homogeneous magnetic field. The dimensions of one channel are 58.5 mm (length) × 1.0 mm (width) × 0.2 mm (height), corresponding to a total volume of 11.7 µL. The reactor volume of 10 µL, however, was determined by the magnetic zone induced by the Nd magnets arranged underneath. Loading of typically 4.5 mg MB Co^{2+} led to a filled reactor volume of approximately 7 µL. Given this volume and a flow rate of 1 µL min^{-1}, the typical residence time was 7 min. Although the performance of packed bed reactors depends on the particle packing and liquid flow patterns, we used the maximum reactor volume of 10 µL to calculate the space time yield (STY) for a simplified approach and to allow comparison with earlier work [24, 48]. The filled channels were connected with short PTFE tubing (internal diameter 0.5 mm) using Mini Luer plugs (microfluidic ChipShop). The same tubing and plugs were used to connect the inlet of the assembled chip with the syringes containing the cofactor/substrate solution controlled by a CETONI neMESYS base module and the outlet with the CETONI Compact Positioning System rotAXYS. The system was controlled by the QmixElements software. The HT200 temperature controlled chipholder (ibidi GmbH, Germany) was set to hold 30 °C. The syringe pumps were filled with 5 mL of the reaction mixture (Sect. 2.4) supplemented with 0.01 % sodium azide to avoid fouling. The chip outflow was automatically fractionated by the rotAXYS system into a 96 well plate, which contained 50 µL 7 M NaClO to stop all enzymatic reactions. The samples were subsequently analyzed by chiral HPLC (Sect. 2.7).

2.7 Chiral HPLC Analysis

Synthesis and characterization of NDK **1** and the analysis of the reaction products by chiral HPLC were performed as previously described [49]. In brief, ethyl acetate extracts from the reaction mixtures (described above) were dried and resuspended in 100 µL of the mobile phase (90 % *n* heptane, 10 % 2 propanol) and 10 30 µL of the solution was analyzed by chiral HPLC (Agilent 1260 series HPLC equipped with a diode array detector (210 nm) on a Lux 3μ Cellulose 1 (150×2.00 mm) chiral column (Phenomenex)). Specific running conditions were used for the analysis of the hydroxy ketones **2** (method A: chromatography solvent 90 % *n* heptane/10 % 2 propanol, 10 min isocratic, a column oven temperature of 10 °C and a flow rate of 0.5 mL min^{-1}) and for the diols **3** (method B: chromatography solvent 98 % *n* heptane/2 % 2 propanol, 20 min isocratic, a column oven temperature of 45 °C and a flow rate of 1.0 mL min^{-1}).

3 Results and Discussion

3.1 Expression, Purification, and Characterization of the Oxidoreductases

To explore and validate the utility of the His/Co^{2+} system for microfluidic biocatalysis, we chose a stereoselective ketoreductase (KRED), the (*R*) selective alcohol dehydrogenase LbADH (EC 1.1.1.2) from *Lactobacillus brevis* ATCC 14869 (Taxonomy ID: 649758). As the substrate, we used the prochiral C_S symmetrical NDK **1**, which can be reduced, depending on the KRED selectivity, either on one or on both of the two carbonyl functions to create four different stereoisomers of hydroxy ketones **2** or diols **3**, respectively (Fig. 2 a) [49]. Since all stereoisomeric products can be readily analyzed by chiral HPLC (Fig. 2 b), the enantiogroup differentiating reduction of the prochiral NDK **1** is ideally suited to evaluate and quantitatively analyze the biocatalytic activity of the LbADH. To cope with the high demand for the structurally complex and expensive KRED cofactor, nicotinamide adenine dinucleotide phosphate (NADPH), two options were conceivable. The most simple approach uses the ability of LbADH to regenerate its own cosubstrate through the oxidation of 2 propanol to acetone [50] (route I in Fig. 2). However, since the LbADH productivity was found to be lower because of the additional oxidation step [24], we used the NADP(H) regeneration enzyme (NRE) GDH (EC 1.1.1.47) from *Bacillus subtilis* subsp. *natto* (Taxonomy ID:

86029) in order to supply the cofactor in situ (route II in Fig. 2). In comparison to other NRE systems, such as formate/lactate decarboxylases, GDH does not produce CO_2 gas bubbles, which are detrimental for microfluidic processes.

The His tagged LbADH and GDH enzymes were cloned, heterologously overexpressed in *E. coli* and purified to homogeneity using IMAC as previously described [25]. The purity of the enzymes was found to be >95 %, as determined by SDS PAGE with subsequent Coomassie staining (Fig. 3).

Next, the reaction kinetics and stereoselectivity for the conversion of NDK **1** into the hydroxyketone **2** and diol **3** products by the purified enzymes in solution was analyzed by chiral HPLC. As expected, the (*R*) selective LbADH His produced the (*R*) syn/anti hydroxyketones **2c/d** (e.r. > 99:1; d.r. ~60:40), which were then rapidly further reduced to form the pseudo C_2 diol **3d**. The specific activities of the enzymes are shown in Tab. 1.

We chose a flow rate of 1 µL min^{-1}, leading to the typical residence time of 7 min, as well as the typical enzyme ratio and particle loading (discussed below in Sect. 3.3) to allow the direct comparison with the previously described packed bed reactor [24]. The in depth comparison of the enzymatic activities in solution revealed that the His LbADH variant showed a 13 % lower activity than a previously described LbADH variant with a 39 amino acid SBP tag [24] and a 30 % higher activity than an LbADH variant [25] that contained the 113 amino acid SpyCatcher domain for specific immobilization. The purified GDH His enzyme variant showed a more than threefold higher specific activity than a previously described GDH SBP variant [24]; however, the activity was still 20 % lower than that of a variant fused with the SpyTag (13 amino acid) peptide [25]. Although all enzyme activities found here are in the same order of magnitude, the slight changes nevertheless clearly emphasize that genetic fusion is often accompanied by changes in the specific activity.

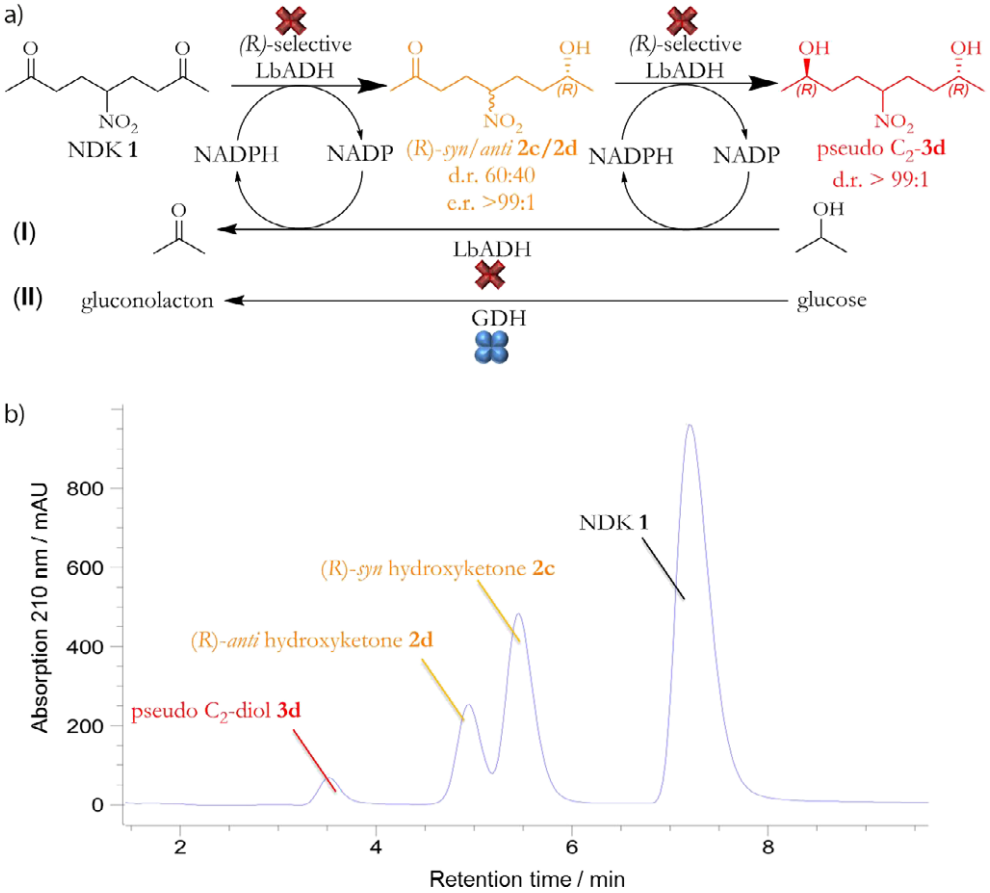

Figure 2. (*R*)-selective reduction of the prochiral C_s-symmetrical NDK **1** by LbADH. (a) NDK **1** reduction employing different methods for NADPH cofactor regeneration. Note that for the sake of simplicity, only (*R*)-selective reaction products are shown; for the structure of the corresponding (*S*)-selective reaction products, i.e., the syn/anti-hydroxyketones **2a**/**2b** and the (*S*,*S*)-pseudo-C_2-diol **3c** or the *meso*-syn/anti-diols **3a**/**3b**, see [49]. The NADPH cofactor can be regenerated either by the LbADH-mediated oxidation of 2-propanol to acetone (route I) or by the "helper"-enzyme glucose dehydrogenase (GDH), which is oxidizing glucose to gluconolactone (route II). (b) Exemplary chiral HPLC chromatogram showing the separation of all educts and products of the reduction of NDK to the (*R*)-hydroxyketone **2c**/**2d** and further to the (*R*,*R*)-configured pseudo-C2-diol **3d**.

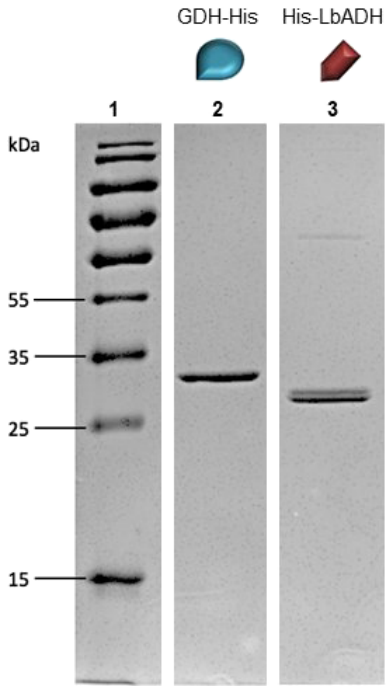

Figure 3. Characterization of the enzymes GDH-His and His-LbADH using a Coomassie-stained SDS-polyacrylamide gel. Lane 1: PageRuler Prestained Protein Ladder Plus (Thermo Scientific); lane 2: GDH-His (29 kDa), lane 3: His-LbADH (27.6 kDa).

3.2 Immobilization of the Purified Oxidoreductases on MB

Apart from optimal catalytic activity of the enzymes, maximizing the volumetric activity of flow reactors is of key importance and is determined by the binding capacity of the inner reactor surface and the carrier materials utilized. In our previous work, we utilized Dynabeads microparticles with a diameter of 2.7 µm to increase the reactor surface/binding capacity from approximately 140 mm^2 (empty) to 6700 mm^2 (filled) [24]. By employing beads with a diameter of only 1.0 µm, we here further increase the effective reactor surface by approximately 2 3 fold and thus improve the theoretical enzyme binding capacity.

Next, the specific enzyme binding capacity of the commercially available, Co^{2+} functionalized superparamagnetic MB (MB Co^{2+}) was determined. To this end, MB Co^{2+} were incubated with an excess of the purified enzymes for 30 min and then isolated by magnetic separation. In order to determine the amount of enzyme immobilized on the MB (enzyme@MB), the enzyme functionalized beads were stripped by heating for 10 min at 95 °C in 1 % SDS sample buffer. The amount of removed enzymes was then determined by SDS PAGE. The binding capacity was calculated from comparative greyscale analysis (Fig. 4) and the results are summarized in Tab. 2. The obtained data indicates that similar amounts of 1 ± 0.1 nmol corresponding to 28 ± 2 µg of both enzymes, His LbADH and His GDH, were immobilized per milligram of MB. These results are only 25 % lower than the nominal binding capacity for a monomeric protein of the same size, as given by the supplier. As expected, the application of the smaller beads with a diameter of 1.0 µm resulted in a threefold higher binding capacity than the recently

Table 1. Specific activities of the purified enzymes.

	MW	Specific activity[a)]	
	[$g_{protein}$ $mol_{subunit}^{-1}$]	[µ$mol_{substrate}$ min^{-1} $mg_{protein}^{-1}$]	[µ$mol_{substrate}$ min^{-1} µ$mol_{subunit}^{-1}$)]
His LbADH	27 638	13.4 ± 0.7	371 ± 18
GDH His	29 014	3.7 ± 0.4	106 ± 11

[a)]Specific activities of the purified His LbADH and GDH His using NDK **1** and glucose as substrates. The specific activity data is normalized to protein subunits because LbADH [50] and GDH [55] are homotetramers. The data represent the mean of at least triplicate analyses ± 1 SD (standard deviation).

Table 2. Specific enzyme binding capacity of the MB-Co^{2+} beads and activities of the immobilized enzymes.

	MW	MB Co^{2+} binding capacity[a)]		Specific activity[b)]		
	[$g_{protein}$ $mol_{subunit}^{-1}$]	[µ$g_{protein}$ mg_{MB}^{-1}]	[n$mol_{subunit}$ mg_{MB}^{-1}]	[n$mol_{substrate}$ min^{-1} mg_{MB}^{-1}]	[µ$mol_{substrate}$ min^{-1} $mg_{protein}^{-1}$]	[µ$mol_{substrate}$ min^{-1} µ$mol_{subunit}^{-1}$]
His LbADH@MB Co^{2+}	27 638	30 ± 1	1.1	265 ± 15	8.9 ± 0.5	255 ± 14
GDH His@MB Co^{2+}	29 014	28 ± 1	1.0	14.1 ± 3.8	0.5 ± 0.1	15 ± 4

[a)]MB Co^{2+} binding capacity analyzed by comparative greyscale analysis shown in Fig. 4. The bead binding capacity data is normalized to protein subunits because LbADH [50] and GDH [55] are homotetramers. The data represent the mean of at least triplicate analyses ± 1 SD (standard deviation).
[b)]Specific activities of immobilized His LbADH and GDH His, determined by using NDK **1** and glucose as substrates. The data represent the mean of at least triplicate analyses ± 1 SD.

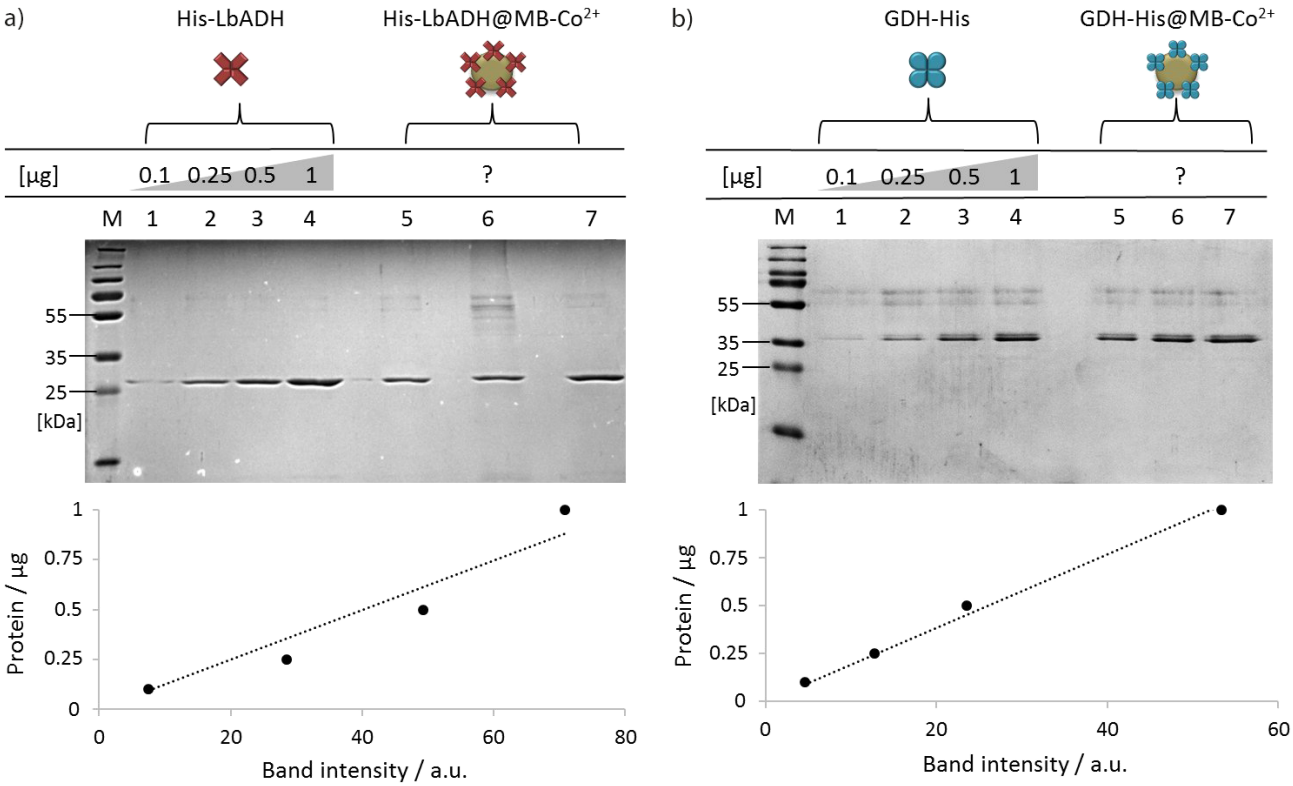

Figure 4. Specific MB-Co^{2+} bead binding capacity for the enzymes His-LbADH (a) and GDH-His (b) analyzed by comparative greyscale analysis. The amount of protein on the MB (lanes 5 7) was determined by comparison with the band intensities of proteins with known concentrations (lanes 1 4; M: protein ladder).

described 2.7 µm diameter streptavidin coated beads (MB STV) [24].

In a next step, the catalytic activities of the enzyme functionalized beads were determined by chiral HPLC. The results are shown in Tab. 2. We found that the specific activity of the His LbADH@MB Co^{2+} beads was more than threefold higher than that of the previously described LbADH SBP@MB STV. This correlates with the approximately 2 3 fold higher binding capacity. However, despite the higher binding capacity, the GDH His@MB Co^{2+} beads only showed a 75 % higher activity than GDH SBP@MB STV. This result suggested that immobilization of the GDH His on the MB Co^{2+} beads led to a reduction of the enzyme's activity.

Indeed, careful analysis and comparison of enzymatic activities in either the free or bound state indicated that the activity of the bead immo bilized enzymes was reduced (Fig. 5). MB immobi lized His LbADH had a residual activity of 69 %, whereas the immobilized GDH His showed a residual activity of only 14 %. It is important to note that the previously described immobilization of these enzymes via the SBP tag or the HOB tag only led to a slight decrease in activity of 20 %. The observed differences in the activity of immobilized enzyme could be caused either by sterical hin drance and blocked active sites in the more tightly packed enzymes on the Co^{2+} beads or by a changed local environment

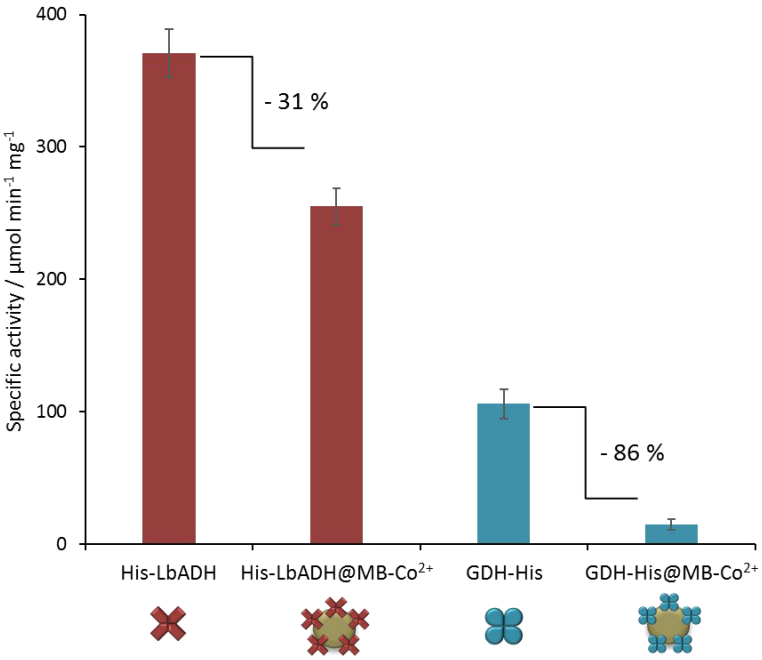

Figure 5. Specific activity of free and MB-immobilized enzymes. Data and error bars represent the mean of triplicate analyses.

of the enzymes on these beads. Despite the loss of activity, both types of enzyme functionalized beads were fully functional and could thus be used in microfluidic flow through systems.

3.3 Application of Self-Immobilizing Oxidoreductases in Miniaturized Flow Reactors

To study the performance of self immobilizing His tagged fusion enzymes, we used the previously described compartmentalized microfluidic packed bed reactor, which can be conveniently loaded with magnetic beads (Fig. 1). The microfluidic packed bed reactor consists of a PMMA chip that contains four microchannels, each with a volume of about 10 µL (Fig. 1) [51]. The chip had rectangular Nd magnets located underneath the microchannels to retain the superparamagnetic beads, which were loaded by simple infusion of a bead suspension. The channels were each loaded with 4.5 mg of a mixture of microbeads, containing 4 mg GDH His@MB Co^{2+} and 0.5 mg His LbADH@MB Co^{2+}. This 8:1 ratio of enzyme coated microbeads was used to allow a comparison with the previously described packed bed reactor and to compensate for the differences in catalytic turnover between GDH and LbADH [24]. The so assembled microreactor was operated at a flow rate of 1 µL min^{-1} at 30 °C for up to 109 h. The educt/product distribution in the outflow of the reactor was determined via chiral HPLC analysis (Fig. 6). In the first two days, the reactor showed an average overall NDK conversion of 98 % to form 8 % (*R*) syn/anti hydroketone **2c/d** with 90 % of the wanted diol **3d** product, resulting in a diol STY of 131 g $L^{-1}day^{-1}$. This STY was > 30 % higher than that of the previously described packed bed reactor with larger beads [24] (Tab. 3). However, due to higher amounts of protein in the channels, the specific productivity (about 1.0 g $L_{reactor\ volume}^{-1}day^{-1}\mu g_{protein}^{-1}$] was only less than 50 % of that observed in the previous study [24]. Most likely, the lower specific productivity, as compared to the other systems, is due to the lower apparent activity of the immobilized enzymes. The reason for this is likely the crowding effect triggered by the high protein loadings. This could lead to mass transport limitations for the substrates to access the immobilized active sites. In general, however, as indicated in Tab. 3, all the evaluated binding tags (His, SBP, Halo or HOB) are well suited for the fabrication of flow biocatalysis reactors. In agreement with the previous comparison of SBP versus HOB [24], no substantial leakage of bound proteins occurs during reactor operation. Hence, the present study confirms that enzyme microreactors based on non covalent immobilization techniques exhibit a high process stability that is at least as good as that observed for covalent enzyme immobilization.

4 Conclusion

In conclusion, we herein demonstrate that oxidoreductases equipped with the commonly used His tag can be employed as self immobilizing biocatalysts in miniaturized packed bed flow reactors. With this approach, enzymes can be used without extensive purification and the reactor can be assembled from commercially available standard parts, thereby significantly reducing time and cost for the development of new catalytic reactions. We here used the industrially relevant LbADH for stereoselective syntheses of chiral alcohols. However, our concept should also be applicable to many other industrially relevant enzymes, such as imine reductases [52], P450 monooxygenases [53], or transaminases [54]. We therefore anticipate that flow reactors equipped with self immobilizing biocatalysts could be of tremendous utility for the future development of sustainable production processes.

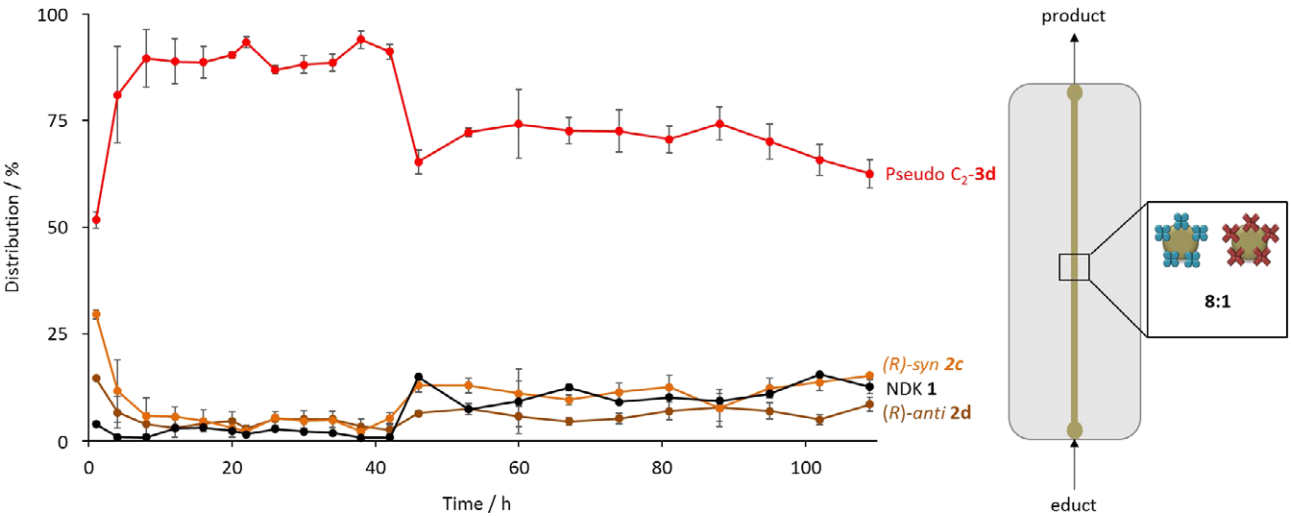

Figure 6. Stereoselective reduction of NDK **1** to (*R*)-syn/anti-hydroketone **2c/d** and diol **3d** in a microfluidic packed-bed reactor. The chip configuration scheme is shown next to the product formation graph, indicating that the channel contained His-LbADH@MB-Co^{2+} and GDH-His@ MB-Co^{2+} in a ratio of about 8:1. The graphs illustrate the educt/product distribution determined by chiral HPLC in the outflow of the reactor. Note that the drop in product formation at 46 h was caused by the exchange of the substrate solution. The data and error bars represent the mean of triplicate analyses.

Table 3. Comparison of process parameters.

KRED	Ref.	Product formation[a)] [%]	STY[a)] [$g_{product}\ L_{reactor\ volume}^{-1} day^{-1}$]	Protein loading per channel [µg]	Specific productivity[a)] [$g_{product}\ L_{reactor\ volume}^{-1} day^{-1} \mu g_{protein}^{-1}$]
Gre2p SBP	[24]	73	106	47	2.3
Gre2p HOB	[24]	66	96	34	2.8
Gre2p ST[b)]	[24]	54	79		
LbADH SBP	[24]	63	92	42	2.2
LbADH His	this study	90	131	127	1.0

[a)]Average product formation measured in the reactor outflow over the first two days. In the case of the KRED Gre2p, (*S*) anti hydroxyketone **2b**, and for the KRED LbADH, (*R*,*R*) configured pseudo C2 diol **3d** was defined as the product. [b)]The quantitative comparison of immobilized and free Gre2p ST was not possible because the covalent ST/SC binding prevented stripping and thus quantification of the amount of bead bound protein.

Acknowledgment

This research was funded by the Helmholtz program "BioInterfaces in Technology and Medicine" and the DFG project Ni399/15 1. P.B. is grateful for a Kekulé fellowship by the Fonds der Chemischen Industrie. We thank Anke Dech for help with the protein purification.

The authors have declared no conflict of interest.

Abbreviations

d.r.	diastereomeric ratio
e.r.	enantiomeric ratio
GDH	glucose dehydrogenase
His	hexahistidine
HOB	Halo based oligonucleotide binder
HPLC	high performance liquid chromatography
IMAC	immobilized metal affinity chromatography
IPTG	isopropyl β d 1 thiogalactopyranoside
KRED	ketoreductase
LbADH	(*R*) selective alcohol dehydrogenase from *Lactobacillus brevis*
MB	magnetic bead
MWCO	molecular weight cut off
$NADP^+$/NADPH	oxidized/reduced nicotinamide adenine dinucleotide phosphate
NDK	5 nitrononane 2,8 dione
NRE	NADP(H) regeneration enzyme
NTA	nitrilotriacetic acid
OD	optical density
PAGE	polyacrylamide gel electrophoresis
PMMA	polymethylmethacrylate
PTFE	polytetrafluoroethylene
SBP	streptavidin binding peptide
SC	SpyCatcher
SDS	sodium dodecyl sulfate
STV	streptavidin
STY	space time yield

References

[1] A. J. Straathof, *Chem. Rev.* **2014**, *114*, 1871 1908. DOI: https://doi.org/10.1021/cr400309c

[2] C. Han, S. Savage, M. Al Sayah, H. Yajima, T. Remarchuk, R. Reents, B. Wirz, H. Iding, S. Bachmann, S. M. Fantasia, M. Scalone, A. Hell, P. Hidber, F. Gosselin, *Org. Lett.* **2017**, *19*, 4806 4809. DOI: https://doi.org/10.1021/acs.orglett.7b02228

[3] J. Liang, J. Lalonde, B. Borup, V. Mitchell, E. Mundorff, N. Trinh, D. A. Kochrekar, R. N. Cherat, G. G. Pai, *Org. Process Res. Dev.* **2010**, *14*, 193 198. DOI: https://doi.org/10.1021/op900272d

[4] S. K. Ma, J. Gruber, C. Davis, L. Newman, D. Gray, A. Wang, J. Grate, G. W. Huisman, R. A. Sheldon, *Green Chem.* **2010**, *12*, 81 86. DOI: https://doi.org/10.1039/b919115c

[5] C. K. Savile, J. M. Janey, E. C. Mundorff, J. C. Moore, S. Tam, W. R. Jarvis, J. C. Colbeck, A. Krebber, F. J. Fleitz, J. Brands, P. N. Devine, G. W. Huisman, G. J. Hughes, *Science* **2010**, *329*, 305 309. DOI: https://doi.org/10.1126/science.1188934

[6] P. N. Devine, R. M. Howard, R. Kumar, M. P. Thompson, M. D. Truppo, N. J. Turner, *Nat. Rev. Chem.* **2018**, *2*, 409 421. DOI: https://doi.org/10.1038/s41570 018 0055 1

[7] I. Wheeldon, S. D. Minteer, S. Banta, S. C. Barton, P. Atanas sov, M. Sigman, *Nat. Chem.* **2016**, *8*, 299 309. DOI: https://doi.org/10.1038/nchem.2459

[8] A. Kuchler, M. Yoshimoto, S. Luginbuhl, F. Mavelli, P. Walde, *Nat. Nanotechnol.* **2016**, *11*, 409 420. DOI: https://doi.org/10.1038/nnano.2016.54

[9] Z. Chen, A. P. Zeng, *Curr. Opin. Biotechnol.* **2016**, *42*, 198 205. DOI: https://doi.org/10.1016/j.copbio.2016.07.007

[10] K. S. Rabe, J. Muller, M. Skoupi, C. M. Niemeyer, *Angew. Chem., Int. Ed.* **2017**, *56*, 13574 13589. DOI: https://doi.org/10.1002/anie.201703806

[11] S. P. France, L. J. Hepworth, N. J. Turner, S. L. Flitsch, *ACS Catal.* **2017**, *7*, 710 724. DOI: https://doi.org/10.1021/acscatal.6b02979

[12] M. B. Quin, K. K. Wallin, G. Zhang, C. Schmidt Dannert, *Org. Biomol. Chem.* **2017**, *15 (29)*, 4260 4271. DOI: https://doi.org/10.1039/c7ob00391a

[13] J. Britton, S. Majumdar, G. A. Weiss, *Chem. Soc. Rev.* **2018**, *47 (15)*, 5891 5918. DOI: https://doi.org/10.1039/C7CS00906B

[14] M. P. Thompson, I. Peñafiel, S. C. Cosgrove, N. J. Turner, *Org. Process Res. Dev.* **2019**, *23 (1)*, 9 18. DOI: https://doi.org/10.1021/acs.oprd.8b00305

[15] C. Schmid Dannert, F. Lopez Gallego, *Curr. Opin. Chem. Biol.* **2018**, *49*, 97 104. DOI: https://doi.org/10.1016/j.cbpa.2018.11.021

[16] S. Gandomkar, A. Żądło Dobrowolska, W. Kroutil, *Chem CatChem* **2019**, *11*, 225 243. DOI: https://doi.org/10.1002/cctc.201801063

[17] B. P. Mason, K. E. Price, J. L. Steinbacher, A. R. Bogdan, D. T. McQuade, *Chem. Rev.* **2007**, *107*, 2300 2318. DOI: https://doi.org/10.1021/cr050944c

[18] R. Wohlgemuth, I. Plazl, P. Znidarsic Plazl, K. V. Gernaey, J. M. Woodley, *Trends Biotechnol.* **2015**, *33*, 302 314. DOI: https://doi.org/10.1016/j.tibtech.2015.02.010

[19] D. Kim, A. E. Herr, *Biomicrofluidics* **2013**, *7*, 041501. DOI: https://doi.org/10.1063/1.4816934

[20] S. Fornera, P. Kuhn, D. Lombardi, A. D. Schluter, P. S. Dit trich, P. Walde, *ChemPlusChem* **2012**, *77*, 98 101. DOI: https://doi.org/10.1002/cplu.201100068

[21] C. R. Boehm, P. S. Freemont, O. Ces, *Lab Chip* **2013**, *13*, 3426 3432. DOI: https://doi.org/10.1039/c3lc50231g

[22] H. Schroeder, L. Hoffmann, J. Muller, P. Alhorn, M. Fleger, A. Neyer, C. M. Niemeyer, *Small* **2009**, *5*, 1547 1552. DOI: https://doi.org/10.1002/smLl.200801016

[23] T. Peschke, K. S. Rabe, C. M. Niemeyer, *Angew. Chem., Int. Ed.* **2017**, *56*, 2183 2186. DOI: https://doi.org/10.1002/anie.201609590

[24] T. Peschke, M. Skoupi, T. Burgahn, S. Gallus, I. Ahmed, K. S. Rabe, C. M. Niemeyer, *ACS Catal.* **2017**, *7*, 7866 7872. DOI: https://doi.org/10.1021/acscatal.7b02230

[25] T. Peschke, P. Bitterwolf, S. Gallus, Y. Hu, C. Oelschlaeger, N. Willenbacher, K. S. Rabe, C. M. Niemeyer, *Angew. Chem., Int. Ed.* **2018**, *57 (52)*, 17028 17032. DOI: https://doi.org/10.1002/anie.201810331

[26] A. D. Keefe, D. S. Wilson, B. Seelig, J. W. Szostak, *Protein Expression Purif.* **2001**, *23*, 440 446. DOI: https://doi.org/10.1006/prep.2001.1515

[27] B. Zakeri, J. O. Fierer, E. Celik, E. C. Chittock, U. Schwarz Linek, V. T. Moy, M. Howarth, *Proc. Natl. Acad. Sci. U. S. A.* **2012**, *109*, E690 E697. DOI: https://doi.org/10.1073/pnas.1115485109

[28] G. V. Los, K. Wood, *Methods Mol. Biol.* **2007**, *356*, 195 208. DOI: https://doi.org/10.1021/cb800025k

[29] K. J. Kossmann, C. Ziegler, A. Angelin, R. Meyer, M. Skoupi, K. S. Rabe, C. M. Niemeyer, *ChemBioChem* **2016**, *17*, 1102 1106. DOI: https://doi.org/10.1002/cbic.201600039

[30] J. Dobber, T. Gerlach, H. Offermann, D. Rother, M. Pohl, *Green Chem.* **2018**, *20*, 544 552. DOI: https://doi.org/10.1039/c7gc03225k

[31] J. Dobber, M. Pohl, S. V. Ley, B. Musio, *React. Chem. Eng.* **2018**, *3*, 8 12. DOI: https://doi.org/10.1039/c7re00173h

[32] D. Valikhani, J. M. Bolivar, M. Viefhues, D. N. McIlroy, E. X. Vrouwe, B. Nidetzky, *ACS Appl. Mater. Interfaces* **2017**, *9*, 34641 34649. DOI: https://doi.org/10.1021/acsami.7b09875

[33] I. T. Dorn, K. R. Neumaier, R. Tampe, *J. Am. Chem. Soc.* **1998**, *120*, 2753 2763. DOI: https://doi.org/10.1021/ja9735620

[34] V. M. Bolanos Garcia, O. R. Davies, *Biochim. Biophys. Acta, Gen. Subj.* **2006**, *1760*, 1304 1313. DOI: https://doi.org/10.1016/j.bbagen.2006.03.027

[35] K. Terpe, *Appl. Microbiol. Biotechnol.* **2003**, *60*, 523 533. DOI: https://doi.org/10.1007/s00253 002 1158 6

[36] J. M. Bolivar, J. Wiesbauer, B. Nidetzky, *Trends Biotechnol.* **2011**, *29*, 333 342. DOI: https://doi.org/10.1016/j.tibtech.2011.03.005

[37] A. A. Halim, N. Szita, F. Baganz, *J. Biotechnol.* **2013**, *168*, 567 575. DOI: https://doi.org/10.1016/j.jbiotec.2013.09.001

[38] H. Yamaguchi, T. Honda, M. Miyazaki, *J. Flow Chem.* **2016**, *6*, 13 17. DOI: https://doi.org/10.1556/1846.2015.00039

[39] J. Britton, R. P. Dyer, S. Majumdar, C. L. Raston, G. A. Weiss, *Angew. Chem., Int. Ed.* **2017**, *56*, 2296 2301. DOI: https://doi.org/10.1002/anie.201610821

[40] C. Mukai, L. Gao, J. L. Nelson, J. P. Lata, R. Cohen, L. Wu, M. M. Hinchman, M. Bergkvist, R. W. Sherwood, S. Zhang, A. J. Travis, *Angew. Chem., Int. Ed.* **2017**, *56*, 235 238. DOI: https://doi.org/10.1002/anie.201609495

[41] M. L. Contente, F. Paradisi, *Nat. Catal.* **2018**, *1*, 452 459. DOI: https://doi.org/10.1038/s41929 018 0082 9

[42] R. Heinzler, J. Hubner, T. Fischoder, L. Elling, M. Franzreb, *Front. Bioeng. Biotechnol.* **2018**, *6*, 189. DOI: https://doi.org/10.3389/fbioe.2018.00189

[43] K. E. Cassimjee, M. Kadow, Y. Wikmark, M. S. Humble, M. L. Rothstein, D. M. Rothstein, J. E. Backvall, *Chem. Commun.* **2014**, *50*, 9134 9137. DOI: https://doi.org/10.1039/c4cc02605e

[44] W. Bohmer, T. Knaus, A. Volkov, T. K. Slot, N. R. Shiju, K. Engelmark Cassimjee, F. G. Mutti, *J. Biotechnol.* **2019**, *291*, 52 60. DOI: https://doi.org/10.1016/j.jbiotec.2018.12.001

[45] E. Gkantzou, M. Patila, H. Stamatis, *Catalysts* **2018**, *8*, 282. DOI: https://doi.org/10.3390/catal8070282

[46] M. Kearse, R. Moir, A. Wilson, S. Stones Havas, M. Cheung, S. Sturrock, S. Buxton, A. Cooper, S. Markowitz, C. Duran, T. Thierer, B. Ashton, P. Meintjes, A. Drummond, *Bio informatics* **2012**, *28*, 1647 1649. DOI: https://doi.org/10.1093/bioinformatics/bts199

[47] C. A. Schneider, W. S. Rasband, K. W. Eliceiri, *Nat. Methods* **2012**, *9*, 671 675. DOI: https://doi.org/10.1038/nmeth.2089

[48] T. Peschke, P. Bitterwolf, S. Hansen, J. Gasmi, K. S. Rabe, C. M. Niemeyer, *Catalysts* **2019**, *9 (2)*, 164. DOI: https://doi.org.10.3390/catal9020164

[49] M. Skoupi, C. Vaxelaire, C. Strohmann, M. Christmann, C. M. Niemeyer, *Chem. Eur. J.* **2015**, *21*, 8701 8705. DOI: https://doi.org/10.1002/chem.201500741

[50] S. Leuchs, L. Greiner, *Chem. Biochem. Eng. Q.* **2011**, *25*, 267 281.

[51] T. Kampe, A. Konig, H. Schroeder, J. G. Hengstler, C. M. Niemeyer, *Anal. Chem.* **2014**, *86*, 3068 3074. DOI: https://doi.org/10.1021/ac404128k

[52] J. Mangas Sanchez, S. P. France, S. L. Montgomery, G. A. Aleku, H. Man, M. Sharma, J. I. Ramsden, G. Grogan, N. J. Turner, *Curr. Opin. Chem. Biol.* **2017**, *37*, 19 25. DOI: https://doi.org/10.1016/j.cbpa.2016.11.022

[53] V. B. Urlacher, M. Girhard, *Trends Biotechnol.* **2012**, *30*, 26 36. DOI: https://doi.org/10.1016/j.tibtech.2011.06.012

[54] F. Guo, P. Berglund, *Green Chem.* **2017**, *19*, 333 360. DOI: https://doi.org/10.1039/c6gc02328b

[55] W. Hilt, G. Pfleiderer, P. Fortnagel, *Biochim. Biophys. Acta, Protein Struct. Mol. Enzymol.* **1991**, *1076*, 298 304. DOI: https://doi.org/10.1016/0167 4838(91)90281 4